Angewandte
Zuschriften

Heterogeneous Catalysis

DOI: 10.1002/ange.201203462

Watching the Methanol-to-Olefin Process with Time- and Space-Resolved High-Energy Operando X-ray Diffraction**

David S. Wragg, Matthew G. O'Brien, Francesca L. Bleken, Marco Di Michiel, Unni Olsbye, and Helmer Fjellvåg*

The conversion of methanol to olefins (MTO) using zeolite catalysts offers an effective route to valuable chemicals from a low-cost and easily available feedstock.[1] The microporous silicoaluminophosphate zeolite SAPO-34 offers excellent activity and selectivity for this process[2] and has recently come into industrial use. The catalyst framework forms channels defined by windows of eight tetrahedral atoms in the crystallographic a and b directions, allowing access to large elipsoidal cavities with their longest dimension along the c axis. When methanol is converted to hydrocarbons over SAPO-34, only linear products may escape the structure through the narrow windows, while branched and aromatic products are retained in the cavities,[3] eventually forming heavy coke which blocks the pores and deactivates the catalyst. Mechanistic studies of the MTO reaction over SAPO-34 have indicated that the product distribution is governed by product shape selectivity.[4]

Wragg et al. have recently used in situ synchrotron X-ray diffraction methods to study this catalyst under real working conditions in a capillary flow cell.[5] The study revealed that the catalyst expands significantly and asymmetrically (mainly along the crystallographic c axis) during the process because of the formation of reaction intermediates (the hydrocarbon pool, HCP[2,6]). It was also noted that when methanol was sent to the catalyst in pulses each pulse gave a peak in the c-axis length (about 0.5% per pulse) and activity, followed by relaxation of c and loss of activity. This was attributed to the loss of highly active polymethylbenzenes from the HCP as reported by Bleken et al.[7] The link between the formation of HCP intermediates, large coke molecules and c-axis expansion has been further explored with computational methods by Zokaie et al.[8] These studies show that different hydrocarbon molecules inside the cavities causes different levels of expansion: methanol adsorbed at room temperature causes a small (0.5%) contraction in c;[9] while polyaromatics like phenanthrene and pyrene cause an expansion of 3%[8] as observed for deactivated SAPO-34.[5]

Whilst these studies have provided much insight into the MTO process, they rely on single point measurements in small capillary-based systems and therefore lack the dimensions required to understand the operation of processes in larger, more industrial-like reactors. The extra insight given by spatiotemporal measurements has been demonstrated recently for a number of different catalytic systems.[10]

We have used rapid, high-energy X-ray diffraction imaging (HXRD), to study a large (4 mm diameter) fixed MTO reactor bed in situ. The spatiotemporal distribution of the organic species in the catalyst cavities is obtained by measuring the variations of the c-axis structural parameter (as for the capillary flow cell little change in the a axis is observed). To do this we used a setup which allowed us to scan the reactor repeatedly through the X-ray beam (a z-axis scan or z-scan) while the reagent gases flowed (from bottom to top, see the Experimental Section). The experiment was performed on beamline ID15B at the European Synchrotron Radiation Facility (ESRF). The high quality of the rapidly recorded data (1 s time resolution) allows us to map activity as a function of the position in the catalyst bed using unit cell changes determined by Rietveld methods. The product stream was analyzed during the reaction using a mass spectrometer. The results show clear spatiotemporal variation in the reactor and provide important new insights into both the induction period of the reaction and the deactivation of the catalyst which are in turn supported by a novel kinetic model of the MTO process.

A two-dimensional scatter plot of the z-scan results for a sample containing 4% silicon at a flow rate of 30 mL min^{-1} is shown in Figure 1. The results are compared with those obtained for the same sample in a 0.5 mm diameter capillary reactor. This shows that the main features of the capillary reactor results are reproduced in the larger reactor. The basic shape of the curve and the range of expansion are clearly similar in both datasets; however, differences are observed after longer times on stream (TOS), with a huge variation of lattice parameters across the large reactor bed compared to the capillary data. Further details of the validation of the z-scan results against capillary data are given in the Supporting Information.

---

[*] Dr. D. S. Wragg, Dr. F. L. Bleken, Prof. U. Olsbye, Prof. H. Fjellvåg
inGAP Centre for Research-based Innovation and
Centre for Materials and Nanotechnology
Department of Chemistry, University of Oslo
PO box 1033 Blindern, 0315 Oslo (Norway)
E-mail: david.wragg@smn.uio.no
Homepage: http://www.mn.uio.no/ingap/english/

Dr. M. G. O'Brien
Inorganic Chemistry and Catalysis, Utrecht University
Debye Institute for Nanomaterials Science
Universiteitsweg 99, 3584 CG Utrecht (The Netherlands)

Dr. M. Di Michiel
European Synchrotron Radiation Facility
6, Rue Jules Horowitz, 38000 Grenoble (France)

[**] We acknowledge financial support from inGAP and the Norwegian Research Council. The ESRF is thanked for granting beamtime at ID15B. We thank the inGAP MTO group for discussions and SINTEF for the preparation of samples.

Supporting information for this article is available on the WWW under http://dx.doi.org/10.1002/anie.201203462.

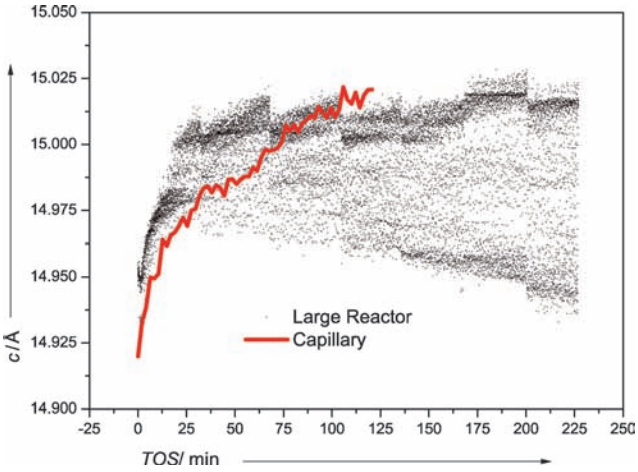

Figure 1. Scatter plot of the z-scan results for the MTO process in a large reactor relative to a line plot from capillary reactor data. The initial expansion and final plateau are reproduced, but a wide range of c-axis values is observed in the dataset of the large reactor at longer times on stream.

When the *z*-scan results are shown in the form of color-scaled contour plots, with the color scale representing the *c*-axis expansion, we see that the range of *c*-axis values observed in Figure 1 has a clear spatial dependence across the reactor bed. Figure 2 shows two different flow rates (50 and 30 mL min^{-1}) for the 4 % silicon sample, while Figure 3 shows the 8 % silicon sample for the first 15 minutes of reaction at 50 mL min^{-1}. The mass spectrometry (MS) data is also plotted on the contour images and demonstrates that whilst the production of propene peaks after around 1–2 minutes depending on the flow rate, it does not drop to zero at the end of the experimental run. Additionally neither the production of dimethyl ether nor the flow-through of unreacted methanol reach a plateau, which together indicate that the catalyst bed is active for MTO conversion throughout the experiment.

Considering first the 50 mL min^{-1} test (Figure 2 a,b), we see that the initial *c*-axis expansion, which we believe corresponds to the formation of HCP species and which is observed as a color change from dark blue to light blue/green in Figure 2, occurs towards the end of the catalyst bed. The expansion then progresses against the reactant flow (Figure 2 b). After 6 minutes on stream, the entire catalyst bed is expanded (green color). With longer times on stream (Figure 1 a), a further expansion (yellow—red color), which we believe corresponds to the formation of heavy polyaromatic coke species, starts 1–2 mm into the catalyst bed, and expands towards the end of the bed with TOS. One of the most fascinating features of the data at longer times on stream is the relaxation of the *c*-axis expansion near to the inlet. This, combined with the large expansion caused by heavy coke,

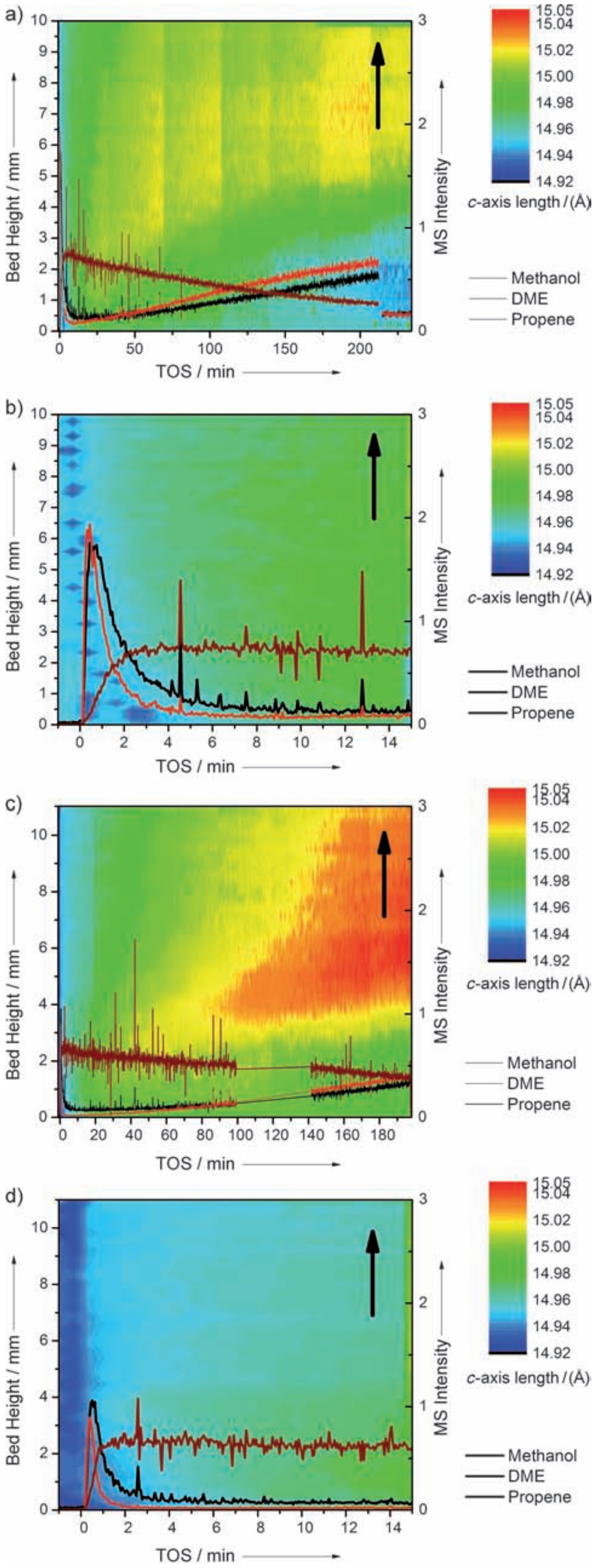

Figure 2. Zeolite SAPO-34 with 4 % silicon at 50 (plots a and b) and 30 mL per minute (plots c and d). The *c*-axis color scale is the same for both flow rates and the direction of reactant flow is indicated by the large black arrows. Plots b and d are enlargements of the first 15 minutes of plots a and c, respectively. An explanation of the steps in plot a is provided in the Supporting Information. The sudden drop in MS intensities in plot a at TOS = 225 minutes is because of an instrument failure (DME = dimethyl ether).

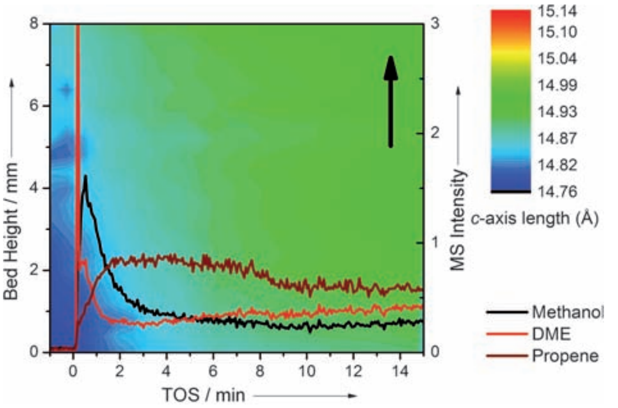

Figure 3. 15 minutes of MTO reaction over 8% silicon SAPO-34 at 50 mL min^{-1}. This sample expands more than the 4% silicon sample and thus the *c*-axis color scale is different to that used in Figure 4. The reactor bed was also shorter because of a shortage of catalyst material. The reactant flow direction is indicated by the large, black arrow.

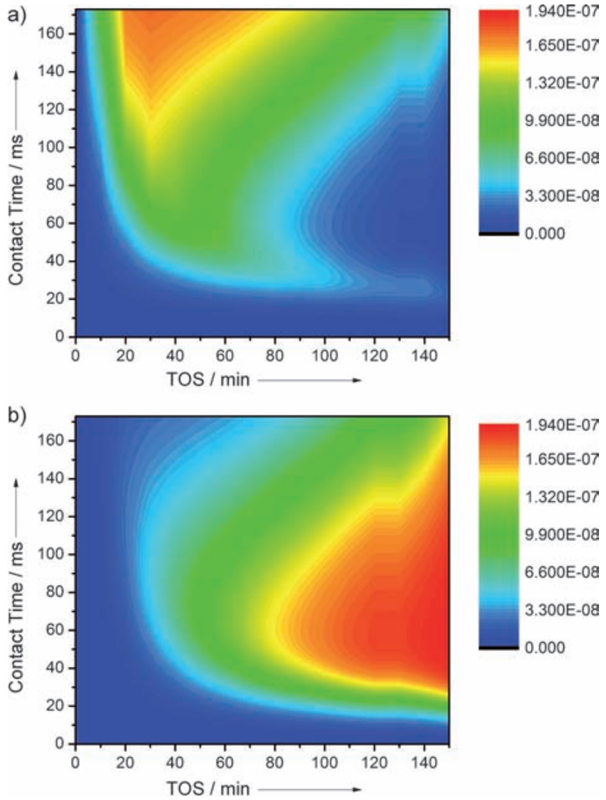

Figure 4. Formation of a) aromatic HCP reaction intermediates and b) coke, from our kinetic model of the MTO process. The initial progress of HCP intermediates towards the bed inlet with TOS is clearly modeled, as is the formation of coke which spreads towards the outlet and causes the final expansion and deactivation.

leads to the large spread of values observed in Figure 1. The relaxation may be related to that observed in pulse feed capillary XRD experiments after each pulse below the point of heavy coke formation.[5]

With a lower feed rate (30 mL min^{-1}, Figure 2c and d), the same global picture is observed. However, the onset of the *c*-axis expansion (Figure 2d) starts earlier in the catalyst bed (approximately 2 mm above the inlet), and expands first against and later with the flow direction before filling the entire bed after 8 minutes on stream. The lower feed rate in this experiment means that each height step of the catalyst bed corresponds to a longer contact time (total contact time = 172 ms) than in the 50 mL min^{-1} experiment (total contact time = 103 ms). The shorter bed length before the onset of expansion for the lower flow rate therefore suggests that the expansion starts after a critical contact time has been reached. At longer times on stream, further expansion occurs, again starting around 2 mm into the bed and expanding towards the outlet with TOS. A larger expansion, suggesting more heavy coke formation, was observed in this case than for the 50 mL min^{-1} experiment. We believe this is also related to the longer contact time at the lower flow rate.

In Figure 3, we see a similar picture of initial bed expansion for the 8% Si sample in the first 15 minutes of the reaction. However, the color scale is different in this case and a direct comparison with the data presented in Figure 2 is difficult. In all cases the beginning of the expansion correlates well with the beginning of propene production (and accompanying decline of methanol and dimethyl ether flow-through) observed in the MS data.

To relate our observations to the reaction we provide a kinetic model based on reaction steps for the formation of propene, monocylic aromatics, and polyaromatic coke molecules from methanol (see the Supporting Information for a full description). The model clearly reproduces the formation and development of the aromatic intermediates (Figure 4a) with TOS, corresponding well with the initial expansion seen in the z-scanning XRD experiments (Figures 2 and 3; green color). The observation that the aromatic HCP fraction is first formed from the middle of the bed and then expands backwards is in agreement with an autocatalytic reaction scheme in which the concentration of active HCP species slowly builds up to a critical level in the direction of the reactor entrance, gradually leading to a high activity even there. As the HCP reacts with methanol to form coke we see the emergence of a coke front (Figure 4b), the shape of which corresponds well with the shape of the final strongly expanded region observed with XRD (Figure 2a and c, red and yellow colors). This is the first kinetic model which explains the importance of methanol in the continued formation of heavy coke and also accounts well for the observed behavior of the catalyst in *z*-scanning XRD. Buildup of the HCP occurs first against the flow of reactants then (in case of surplus HCP free catalyst) with the flow, allowing the olefin production to reach its maximum level.

Based on our observations we propose that the progress of the MTO reaction over SAPO-34 catalysts follows the following course:

1. Formation of the initial HCP at a single point in the reactor which is determined by the flow rate (contact time) and number of catalytic sites, corresponding to a critical concentration of autocatalytic species.
2. Buildup of the HCP, first against the flow of reactants then (in case of surplus HCP free catalyst) with the flow, allowing the olefin production to reach its maximum level.

3. Formation of large coke species. The point where these large coke species appear first depends on the flow rate and the number of catalytic sites. The kinetic model shows that the development of these species agrees well with a reaction scheme in which coke is formed by reaction between methanol and aromatic intermediates.
4. Deactivation of the bed because of heavy coke, yet with some parts of the bed remaining coke free.

Experimental Section

SAPO-34 catalysts containing 4 and 8% silicon (Si/(Si+Al+P)) obtained from SINTEF Oslo were pressed into pellets and sieved to a size of between 0.25 and 0.42 mm. The pellets (100 mg) were loaded on a quartz frit in a fixed bed quartz tube reactor of 4 mm internal diameter. Reaction gases (helium, 20% oxygen in helium, or helium bubbled through methanol held at 19.5 °C) were fed upwards through the frit at a flow rate of either 30 or 50 mL min^{-1} (weight hourly space velocity, WHSV = 3.6 or 5.7 g MeOH g^{-1} catalyst h^{-1}, respectively). The reactor was heated with two Leister LE mini heat guns fitted with heat spreaders. The temperature profile across the bed was measured using a thermocouple inserted into the center of a sample of the catalyst and varied between 346 and 338 °C at the bottom and top of the reactor. The product stream was analyzed using a European Spectrometry Systems ecoSys-P Man-Portable mass spectrometer with capillary inlet and heated inlet tubes.

Hard X-ray diffraction (HXRD) data were collected at beamline ID15B of the European Synchrotron Radiation Facility (ESRF) with a wavelength of 0.14257 Å (89.965 KeV), using a Pixium area detector[11] at a sample–detector distance of 1473 mm. The reactor and heat guns were mounted on a Huber stage capable of very fast translations in the z direction as well as x and y translations. A Huber goniometer head was used for alignment and phi rotations. During data collection the reactor was moved down through the beam at a rate of 0.5 mm s^{-1} with diffractograms being acquired every second, the reactor was then moved back up in one second between scans with no data collection. A sketch representation of this process is shown in the Supporting Information.

The data were radially integrated using DATASQUEEZE to give 2D powder patterns with a 2Θ range from 0 to 10°, and the data were analyzed using parametric Rietveld refinements[12] in TOPAS academic.[13] The large number of datasets meant that it was not possible to process all of the data from each run in a single parametric refinement. Thus, the data were processed in batches of approximately 1450 diffractograms. Further details on the Rietveld refinement process and fitting results are given in the Supporting Information.

Received: May 4, 2012

Keywords: heterogeneous catalysis · industrial chemistry · reaction mechanisms · X-ray diffraction · zeolites

[1] M. Stöcker, *Microporous Mesoporous Mater.* **1999**, *29*, 3–48.
[2] U. Olsbye, M. Bjørgen, S. Svelle, K.-P. Lillerud, S. Kolboe, *Catal. Today* **2005**, *106*, 108–111.
[3] S. Wilson, P. Barger, *Microporous Mesoporous Mater.* **1999**, *29*, 117–126.
[4] B. P. C. Hereijgers, F. Bleken, M. H. Nilsen, S. Svelle, K.-P. Lillerud, M. Bjørgen, B. M. Weckhuysen, U. Olsbye, *J. Catal.* **2009**, *264*, 77–87.
[5] D. S. Wragg, R. E. Johnsen, M. Balasundaram, P. Norby, H. Fjellvåg, A. Grønvold, T. Fuglerud, J. Hafizovic, Ø. B. Vistad, D. Akporiaye, *J. Catal.* **2009**, *268*, 290–296.
[6] a) I. M. Dahl, S. Kolboe, *Catal. Lett.* **1993**, *20*, 329–336; b) I. M. Dahl, S. Kolboe, *J. Catal.* **1994**, *149*, 458–464.
[7] F. Bleken, M. Bjørgen, L. Palumbo, S. Bordiga, S. Svelle, K.-P. Lillerud, U. Olsbye, *Top. Catal.* **2009**, *52*, 218–228.
[8] M. Zokaie, D. S. Wragg, O. Swang, K. P. Lillerud, submitted manuscript.
[9] D. S. Wragg, R. E. Johnsen, P. Norby, H. Fjellvåg, *Microporous Mesoporous Mater.* **2010**, *134*, 210–215.
[10] a) H. Schulz, *Catal. Today* **2010**, *154*, 183–194; b) L. Espinosa-Alonso, M. G. O'Brien, S. D. M. Jacques, A. M. Beale, J. de Jong, P. Barnes, B. M. Weckhuysen, *J. Am. Chem. Soc.* **2009**, *131*, 16932–16938; c) M. G. O'Brien, A. M. Beale, S. D. M. Jacques, M. Di, B. M. Weckhuysen, *ChemCatChem* **2009**, *1*, 99–102; d) M. G. O'Brien, S. D. M. Jacques, M. D. Michiel, P. Barnes, B. M. Weckhuysen, A. M. Beale, *Chem. Sci.* **2012**, *3*, 509–523; e) J.-D. Grunwaldt, B. Kimmerle, A. Baiker, P. Boye, C. G. Schroer, P. Glatzel, C. N. Borca, F. Beckmann, *Catal. Today* **2009**, *145*, 267–278; f) A. M. Beale, S. D. M. Jacques, B. M. Weckhuysen, *Chem. Soc. Rev.* **39**, 4656–4672; g) M. G. O'Brien, A. M. Beale, S. D. M. Jacques, T. Buslaps, V. Honkimaki, B. M. Weckhuysen, *J. Phys. Chem. C* **2009**, *113*, 4890–4897.
[11] J. E. Daniels, M. Drakopoulos, *J. Synchrotron Radiat.* **2009**, *16*, 463–468.
[12] G. W. Stinton, J. S. O. Evans, *J. Appl. Crystallogr.* **2007**, *40*, 87–95.
[13] A. A. Coelho, Bruker AXS, **2006**.